IEEE Access
Multidisciplinary | Rapid Review | Open Access Journal

Received 9 January 2024, accepted 25 January 2024, date of publication 6 February 2024, date of current version 12 February 2024.

Digital Object Identifier 10.1109/ACCESS.2024.3359411

RESEARCH ARTICLE

Improved Model-Free Sliding Mode Control of Linear Motor Based on Time-Varying Gain Model-Assisted Linear Extended State Observer

JIAN LIN, WUJIE JIANG, LEI ZHOU, JITING SUN, AND XINYI SONG
Nanjing Institute of Technology, Nanjing 211167, China

Corresponding author: Jian Lin (zdhxlj00777@163.com)

This work was supported by the Major Project of Natural Science Research of Jiangsu Province Colleges and Universities through the Research on Multi-Disturbance Compound Suppression of Linear Servo System Based on Prediction and Sliding Mode Control under Grant 20KJA460010.

ABSTRACT Aiming at the effects of motor parameter ingress and load mutation on the speed control of permanent magnet synchronous linear motor (PMSLM) motors, this paper designs a PMSLM improved model-free sliding-mode speed control strategy based on the variable-gain model-assisted linear expansion observer (TMLESO). First, time-varying gain-based model-assisted linear expansion observer (MLESO) is designed to improve the accuracy of LESO generalized perturbation estimation. Next, the TMLESO is constructed by combining the MLESO and the time-varying function to solve the problem of large initial peaks. Finally, a model-free sliding-mode velocity controller with adaptable boundary layer thickness is constructed to reduce the effect of sliding-mode jitter on velocity tracking and improve the dynamic performance of the system. The effectiveness of the proposed control strategy is analyzed through simulations and experiments.

INDEX TERMS Permanent magnet synchronous linear motor, time-varying gain-based model-assisted linear expansion observer, model-free sliding mode control, boundary layer adaptive.

I. INTRODUCTION

Compared with rotary motors, linear motors directly utilize electromagnetic thrust to achieve linear motion, which has the advantages of high thrust density and fast response speed. Therefore, they are widely used in modern high-precision industrial fields such as semiconductor manufacturing, aerospace and CNC machining. However, uncertainties such as friction, system parameter variations and load perturbations greatly affect the accuracy of the PMSLM due to the elimination of the intermediate drive link. Therefore, suppressing these uncertainties is of great value in improving the speed control performance of the PMSLM.

With the development of control theory, more and more advanced control strategies, such as smooth-mode control, self-resistant control, predictive control, model-free control [1], [2], [3], [4], etc., are gradually applied to the speed control of PMSLM. Sliding mode control is a nonlinear robust control method [5], [6], the key is the design of the sliding mode surface and the sliding mode convergence rate, and many scholars have carried out in-depth research on these two aspects. In [7] designs a global complementary sliding mode surface, which combines the generalized sliding mode surface and the complementary sliding mode surface to design the controller, which weakens the jitter and improves the system accuracy, but the constant thickness of the boundary layer of the switching function reduces the system robustness. In [8] proposes a fast terminal sliding mode control strategy that ensures that the system converges to the sliding mode surface in a finite time, but the singularity problem arises due to the presence of fractional powers. Model-free control methods utilize only the inputs

The associate editor coordinating the review of this manuscript and approving it for publication was Atif Iqbal.

and outputs of the system, reducing the impact of system parameter variations on control performance [9], [10]. In [11] proposes to apply the combination of the model-free method and the differential-free prediction method to linear motors, which improves the robustness of the system control, but fails to eliminate the current prediction error completely. In [12] applies the model-free control method to the current loop control and improves the current response performance of the system, but it is computationally intensive.

In linear motor control, the estimation of unknown perturbations is particularly important, and [13] proposes to use an expansion observer (ESO) for this purpose, but the ESO it uses suffers from a low accuracy of generalized perturbation estimation as well as a too large peak at the initial moment. For the suppression of the initial peak, [14], [15] proposes the use of a time-varying function for the suppression. In [16] designed a dual perturbation observer for the matched and mismatched perturbations present in the system to improve the immunity of the system.

To address the above problems, this paper firstly designs a time-varying gain model-assisted linear expansion observer (TMLESO) to improve the observation accuracy of the generalized perturbations while avoiding the phenomenon of too large initial peaks. Next, an improved model-free sliding mode control method is designed by combining the sliding mode control with the model-free control method and compensating the unknown perturbations observed by TMLESO to the controller. Meanwhile, a sliding mode control method with adaptive boundary layer thickness is proposed for the problem of fixed thickness of boundary layer of traditional saturation function in sliding mode control. Simulation and experimental results show that the method proposed in this paper is practical and feasible, and effectively improves the speed control performance and robustness of the system.

II. MATHEMATICAL MODEL OF PMSLM

The mathematical model of the voltage equation of the table-posted PMSLM in two isochronous rotating coordinate system is given by (1):

$$\begin{cases} u_d = R_s i_d + L_d \dfrac{di_d}{dt} - \dfrac{\pi}{\tau} v L_q i_q \\ u_q = R_s i_q + L_q \dfrac{di_q}{dt} + \dfrac{\pi}{\tau} v L_d i_d + \psi_f \dfrac{\pi}{\tau} v \end{cases} \tag{1}$$

where u_d and u_q represent the dq-axis voltage of the primary winding, respectively; R_s represents the armature resistance; i_d and i_q represent the dq-axis armature current; L_d and L_q represent the dq-axis inductance, respectively; τ represents the pole distance; v represents the kinematic velocity; ψ_f represents the secondary permanent magnet flux linkage.

For the surface-mounted PMSLM, there is $L_d = L_q$, then the electromagnetic thrust equation and the motion balance equation are written as follows, respectively:

$$F_e = \frac{3p_n}{2} \frac{\pi}{\tau} \psi_f i_q \tag{2}$$

$$M\dot{v}(t) = F_e - F_L - B_m v(t) \tag{3}$$

where F_e represents the electromagnetic thrust; p_n represents the number of pole pairs; M represents the mass of the moving part; F_L represents the load thrust; B_m represents the viscous friction coefficient.

Substituting (2) into (3) and simplifying it into a mathematical model about speed, thus it can obtain that

$$\dot{v}(t) = -\frac{B_m}{M} v(t) - \frac{1}{M} F_L + \frac{3p_n \pi \psi_f}{2M\tau} i_q \tag{4}$$

Considering that the internal parameters of the motor will be perturbed with the operation of the motor, at this time, (4) can be further expressed as follows (5):

$$\dot{v}(t) = -\frac{Bm_0 + \Delta Bm}{m} v(t) - \frac{1}{\mathrm{m}} FL + \frac{3Pn\pi(\psi_{f0} + \Delta\psi_f)}{2} iq \tag{5}$$

where B_{m0} and ψ_{f0} represent the nominal values on the motor nameplate; ΔB_m and $\Delta\psi_f$ represent the perturbation of the internal parameters of the motor.

III. DESIGN OF A TIME-VARYING GAIN MODEL-ASSISTED LINEAR EXPANSION OBSERVER

A. DESIGN OF MLESO

According to Eq. (5)

$$\frac{\mathrm{d}v}{\mathrm{d}t} = -m_0 \mathrm{v}(t) + f' + n_0 i_q \tag{6}$$

where $\mathrm{m}_0 = \frac{Bm0+\Delta Bm}{m}$, $n_o = \frac{3Pn\pi(\varphi f 0+\Delta\varphi f)}{2}$, $f' = -\frac{1}{\mathrm{m}} FL$.

Define the state variables $X_{M1} = v$, $X_{M2} = F$, $u = i_q$, and the state equation of the system is obtained from equation (5)

$$\frac{\mathrm{d}v}{\mathrm{d}t} = -m_0 \mathrm{v}(t) + f' + n_0 i_q \tag{7}$$

where: $\dot{X}_{M2}$ is the first order derivative of the total perturbation and y is the system output.

From equation (7), the state space equation of the motor speed control system is given by

$$\begin{cases} \dot{\boldsymbol{X}}_{\mathrm{M}} = \boldsymbol{A}_{\mathrm{M}} \boldsymbol{x}_{\mathrm{M}} + \boldsymbol{B}_{\mathrm{M}} u + E\dot{\boldsymbol{F}}' \\ y = \boldsymbol{C}\boldsymbol{x}_{\mathrm{M}} \end{cases} \tag{8}$$

where: $E = \begin{bmatrix} 0 \\ 1 \end{bmatrix}$, $\boldsymbol{C} = \begin{bmatrix} 1 \\ 0 \end{bmatrix}^T$, $\boldsymbol{X}_{\mathrm{M}} = \begin{bmatrix} X_{M1} \\ X_{M2} \end{bmatrix}$, $\boldsymbol{A}_{\mathrm{M}} = \begin{bmatrix} 0 & 1 \\ 0 & -m_0 \end{bmatrix}$, $\boldsymbol{B}_{\mathrm{M}} = \begin{bmatrix} n_0 \\ -m_0 n_0 \end{bmatrix}$, where X_M, A_M, B_M, are the state change quantity matrix, state matrix and input matrix of the motor speed control system considering parameter perturbation, respectively.

From equation (8), the state space equation of MLESO is obtained as follows

$$\begin{cases} \dot{z}_{\mathrm{M}} = [\boldsymbol{A}_{\mathrm{M}} - \boldsymbol{M}\boldsymbol{C}] z_{\mathrm{M}} + \begin{bmatrix} \boldsymbol{B}_M \boldsymbol{M} \end{bmatrix} \boldsymbol{u}_c \\ y_c = \boldsymbol{C}\boldsymbol{z}_{\mathrm{M}} \end{cases} \tag{9}$$

where: $z_{\mathrm{M}} = [z_1\ z_{\mathrm{M2}}]^{\mathrm{T}}$ is the state vector of the MLESO, which represents the tracking signals of the X_{M1}, which is $z_1 \rightarrow x_{\mathrm{M1}}$, $z_{\mathrm{M2}} \rightarrow x_{\mathrm{M2}}$; $\boldsymbol{M} = \begin{bmatrix} M_1\ M_2 \end{bmatrix}^T$ is the MLESO gain matrix to be designed.

As shown in Eq. (9), compared with the LSEO, MLESO not only considers the two components of unmodeled and external disturbances, but also takes the internal parameter perturbation of the motor into account. When the external environment changes, its influence on the motor operation can be better reduced, thus improving the observation accuracy of the system.

In order to simplify the design process of MLESO, the poles of the observer characteristic equations are configured to the same position (-w$_0$,w$_0$) as the observer bandwidth after parametric calibration so that it satisfies equation (10)

$$\lambda(s) = |s\boldsymbol{I} - (\boldsymbol{A} - \boldsymbol{LC})| = (s + \omega_0)^2 \tag{10}$$

The gain matrix of MLESO can be obtained from Eq. (10)

$$\boldsymbol{M} = \begin{bmatrix} M_1 & M_2 \end{bmatrix}^T \tag{11}$$

where: $\begin{cases} M_1 = 2\omega_0 - m_0 \\ M_2 = \omega_0^2 - 2m_0\omega_0 + m_0^2 \end{cases}$

In order for MLESO to run in MATLAB, the associated algorithm needs to be discretized. In this section, Eq. (9) is discretized using the forward difference method, which is

$$\begin{cases} e_1(k) = z_1(k) - y(k) \\ \dfrac{z_1(k+1) - z_1(k)}{T_s} = z_{M2}(k) - M_{c1}e_1(k) + n_0 u \\ \dfrac{z_{M2}(k+1) - z_{M2}(k)}{T_s} = -m_0\left[z_{M2}(k) + n_0 u\right] - M_{c2}e_1(k) \end{cases} \tag{12}$$

where: T_s is the sampling period;M_{c1}, M_{c2} is the error feedback gain coefficient of the discrete MLESO to be designed.

The characteristic equation of the discrete estimator is as follows:

$$\lambda(z) = |z\boldsymbol{I} - \boldsymbol{\Phi}_E| = (z - \beta)^2 \tag{13}$$

where: $\boldsymbol{\Phi}_E = \begin{bmatrix} 1 - T_s M_{c1} & T_s \\ -T_s M_{c2} & 1 - T_s \mathrm{m}_0 \end{bmatrix}$; β is the pole of the discrete model auxiliary LESO.

The gain matrix of the discrete estimator can be obtained

$$\begin{cases} M_{c1} = \dfrac{2 - 2\beta - T_s m_0}{T_s} \\ M_{c2} = \dfrac{\beta^2 + 2(T_s m_0 - 1)\beta + (1 - T_s m_0)^2}{T_s^2} \end{cases} \tag{14}$$

where: $\beta = e^{-\omega_0 T_s}$.

B. DESIGN OF TIME-VARYING FUNCTIONS

The MLESO designed in Eq. (9) is a high gain observer, which will cause the system to peak too large at the initial moment and even generate oscillation phenomenon. Since the gain of MLESO is a function of the time involved, in this paper, the gain is designed as a time-varying gain. At the initial moment of motor startup, a small gain is designed to suppress the phenomenon of peak oversizing, which gradually increases and stabilizes to a constant value as the motor speed increases. The time-varying function is designed as:

$$L(t) = \begin{cases} \beta 0 + kit, & 0 \le \mathrm{t} < \dfrac{\beta 0 - \mu 0}{ki} \\ \mu 0, & \mathrm{t} \ge \dfrac{\beta 1 - \beta 0}{ki} \end{cases} \tag{15}$$

where $\beta 0$, $\mu 0$ is a constant, ki is the scale factor, t is the time.

IV. IMPROVED MODEL-FREE SLIDING MODE CONTROLLER DESIGD

The traditional sliding mode control is highly dependent on the motor parameters, and the speed tracking performance is reduced when the motor parameters are regulated, for this reason, a model-free sliding mode controller is used in this paper.

A. HYPERLOCAL MODEL-FREE THEORY

The hyperlocal model-free theory relies only on the inputs and outputs of the control system in modeling [17], [18]. Therefore, it can reduce the dependence of the system on the motor parameters and thus improve the overall robust performance.

For a single-input single-output system, the hyperlocal model can be described as the following unknown linear equation:

$$H(ty(t)y(t)' \ldots y(t)^n\, u(t)u(t)' \ldots u(t)^m) = 0 \tag{16}$$

where y is the output of the system; u is the input of the system; and H is a sufficiently smooth function of its parameters.

In general, equation (16) can be abbreviated as

$$y^{(n)} = \rho u + F \tag{17}$$

where n denotes the highest order of the input $y$to the system, typically $n = 1$; $\rho$is a non-physical constant parameter; $y$is the output; u is the input; and F is the known part of the system and all the parameter uncertainties.

B. MODEL-FREE SLIDING MODE CONTROL

In Eq.(17), F contains motor parameters such as motor resistance, inductance, and permanent magnet magnetic chain, however, these parameters are subject to change with the external environment. Therefore, in order to improve the robust performance of the system, the variation of these parameters should be taken into account as well. For this purpose the velocity loop extended hyperlocal null model of PMSLM is designed as:

$$\begin{cases} \dot{v} = \eta i_q^* + F + F' = \eta i_q^* + Y \\ Y = F + F' \end{cases} \tag{18}$$

where, $\eta$is the current coefficient to be designed, $F$is all the uncertain parameters of the system, $F'$is the variation value of$F$, Y is the sum of$F$ andF'. From Eq. (9) and Eq. (12), the total disturbance of the system is obtained in real time byz_{M2}.

From equation (18)

$$\mathrm{i}_q^* = \frac{-Y + \dot{v}^* + u_s}{\eta} \tag{19}$$

where: u_s is the output of the sliding mode controller to be designed.

Defining the velocity error as a state variable yields

$$\dot{e}_3 + u_s = 0 \tag{20}$$

From Eq. (18) and Eq. (19), we get

$$\dot{v}^* - \dot{v} = -u_s \tag{21}$$

The traditional sliding mode control usually adopts linear sliding surface when designing the sliding mode surface, which can achieve the asymptotic convergence of the system state, but the convergence speed is slow. The terminal sliding mode control introduces a nonlinear sliding surface [19], [20], which can well solve the above problems and converge to the equilibrium point in a limited time.

The terminal slide mold surface is designed to:

$$\mathrm{s} = e_3 + a_1 \left|e_4\right|^{\mathrm{r}} sign(e_1) \tag{22}$$

where e_3 is the position error, e_4 is the velocity error, and r is a positive odd number.

Derivation of equation (22) yields

$$\dot{s} = e_1 + r a_1 \left|e_1\right|^{r-1} \dot{e}_1 \tag{23}$$

The traditional convergence rate is away from the sliding mold surface, there is the problem of convergence rate speed is too small, this paper design convergence rate is shown below:

$$\dot{s} = -k_1 s - k_2 \left|s\right|^b sign(s) \tag{24}$$

where: k_1, k_2 both > 0, $0 < \mathrm{b} < 1$.

Combining Eq. (23) and Eq. (24) yields a control output of:

$$u_s = \frac{e_1 + k_1 s + k_2 \left|s\right|^b sign(s)}{r a_1 \left|e_1\right|^{r-1}} \tag{25}$$

Lyapunov functions are used to prove the stability of this velocity controller:

$$V = \frac{1}{2} s^2 \tag{26}$$

Derivation of equation (26) gives:

$$\begin{aligned} \dot{V} &= s\dot{s} \\ &= s(-k_1 s - k_2 \left|s\right|^b sign(s)) \\ &\le \begin{cases} s(-k_1 s - k_2 \left|s\right|^b) & s > 0 \\ 0 & s = 0 \\ s(-k_1 s + k_2 \left|s\right|^b) & s < 0 \end{cases} \end{aligned} \tag{27}$$

In the case that k_1, k_2 are both greater than 0, it can be seen that $\dot{V} \le 0$. Therefore, the convergence rate designed in this paper satisfies the stability condition, the controller has good stability.

C. SWITCHING FUNCTION DESIGN FOR ADAPTIVE BOUNDARY LAYER THICKNESS

The switching function used in Eq. (25) is the sign function sgn(s), which constantly traverses near the sliding mold surface, thus generating a serious vibration phenomenon and affecting the accuracy of speed estimation. In [21] and [22] proposes to use the saturation function sat(s) instead of sgn(s), which can reduce the jitter problem caused by the discontinuity of the sgn(s) function during the switching. However, its boundary layer thickness is fixed. Although the steady-state performance can be guaranteed at a fixed rotational speed, the thickness of the boundary layer cannot be adjusted in real time with the change of working conditions.

In order to reduce the impact of system jitter on the control performance. In this paper, a switching function $S - T(s)$ is proposed in which the thickness of the boundary layer can be changed adaptively with the change of the value of the error in the velocity of the actuator. the expression of this function is shown as follows:

$$S - T(s) = \begin{cases} \mathrm{sgn}(s) & |\mathrm{s}| > f(s_v) \\ 1 - \dfrac{\pi}{e^{f(s_v)s} + 1} & |\mathrm{s}| \le f(s_v) \end{cases} \tag{28}$$

where: $f(s_v) = \phi + \sqrt{\alpha s_v^2 + 1}$ is the value of the change in the velocity of the actuator, is the error coefficient, and is the initial boundary layer thickness.

When s_v =0.1, 0.2, 0.5, the image of $S - T(s)$ function is shown in Fig. 1.

As can be seen from Fig. 1 the thickness of the boundary layer of the $S - T(s)$ function changes with s_v. When s_v is larger, the boundary layer of the continuous function is thicker, and the smaller s_v is, the thickness of the boundary layer is smaller, which is closer to the symbolic function sgn(s). It can be seen that the function $S - T(s)$ can adaptively change the thickness of the boundary layer according to the changing value of the velocity of the actuator, which improves the control performance of the system.

V. SYSTEM SIMULATION VERIFICATION

The overall structural block diagram of the improved model-free sliding mode control system for linear motor based on time-varying gain MLESO is shown in Fig. 2. From the figure below, the variable gain MLESO observes the generalized perturbation F through the velocity v and the q-axis current, and the improved model-free sliding mode controller uses F and the velocity error to obtain the current.

In order to verify the effectiveness of the observer and control strategy proposed in this paper. The PMSLM simulation model is built in MATLAB/Simulink and the vector control scheme with id = 0 is used. Firstly, TMLESO and MLESO are compared to analyze the observation performance of the two methods for generalized perturbations. Then MFSMC and MFSMC with adaptive boundary layer thickness are compared in simulation. Table 1 shows the parameter settings of the permanent magnet synchronous linear motor.

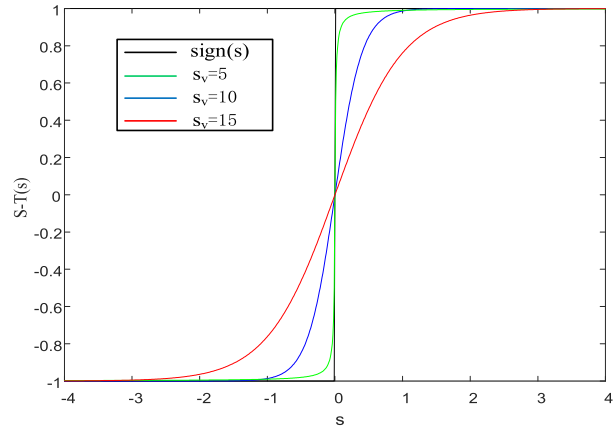

FIGURE 1. Comparison of S-T(s) function with sign(s) function.

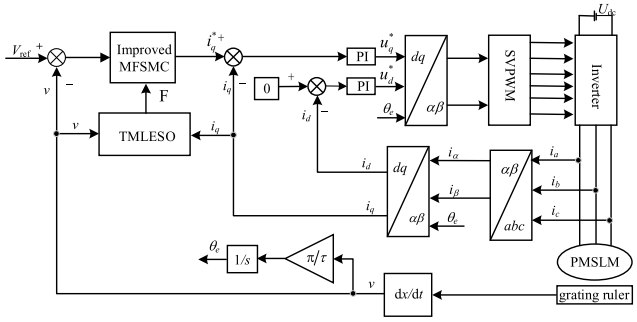

FIGURE 2. Block diagram of improved MFSMC of PMSLM based on TMALESO.

In this paper, the observer and controller parameters are selected as follows: $k_1 = 4, k_2 = 3, a_1 = 0.5, b = 0.3, r = 3, \beta_0 = 3, \mu 0 = 6, \phi = 0.01, \alpha = 0.05$.

The motor is set up to start with no load, given that the linear velocity of the actuator is 0.2 m/s. A load of 100 N is applied abruptly at 0.2 s, and the load is abruptly reduced to 50 N at 0.3 s.

Fig. 3 shows the observed waveforms of TMLESO and conventional LESO for perturbations when parameter perturbation is considered. From Fig. 3, the peak value of the traditional LESO perturbation reaches 47.6N at the initial moment of the motor startup, while the TMLESO is only 1.6N, and the problem of the excessive peak value is effectively solved. Moreover, the amount of perturbation overshoot of TMLESO is smaller than that of conventional LESO during both sudden load addition and subtraction. Therefore, TMLESO is able to more accurately estimate the amount of generalized perturbation and feed it back to the controller compared to the traditional LESO, which effectively improves the control accuracy.

In Fig.3, a represents LESO, b represents TMLESO.

Fig. 4 shows the linear velocity response curves of MFSMC for the two strategies of fixed boundary layer and adaptive boundary layer, respectively. From Fig. 4, it can be seen that the response time of the adaptive boundary layer is 0.01s during the motor startup phase, while the response time of the fixed boundary layer is 0.03s. And the velocity

TABLE 1. Parameters of the PMSLM.

Parameter and unit	Value
the number of pole pairs p_n	2
pole distance τ/mm	60.88
armature resistance R_s/Ω	2.925
Inductance L_d=L_q/mH	8.5
the secondary permanent magnet flux linkage ψ_f/Wb	0.18
the mass of the moving part M/kg	0.68
viscous friction coefficient B_m/N·m·s	0.2

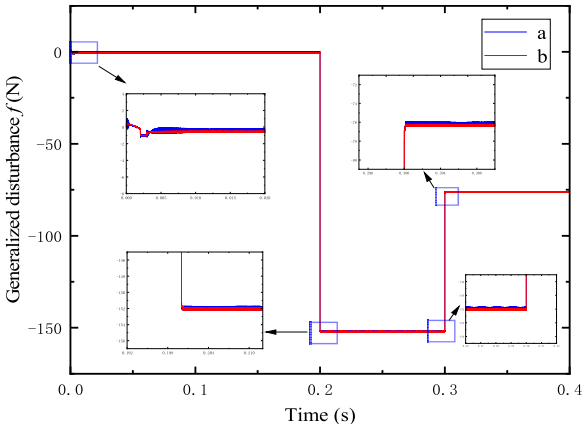

FIGURE 3. Generalized perturbation observation curve.

overshoot with adaptive boundary layer control is only 0.002 m/s, while the velocity overshoot under fixed boundary layer control reaches 0.018 m/s. The time for the adaptive boundary layer to return to the steady state is significantly faster than that of the fixed boundary layer for both 0.2 s sudden load increase and 0.3 s sudden load decrease. The simulation shows that the adaptive boundary layer has better velocity tracking ability and faster dynamic response.

In Fig. 4, a represents MFSMC with fixed boundary layer, b represents MFSMC with adaptive boundary layer.

Fig. 5 shows the velocity error curves for the two control methods considering parameter perturbation, respectively. The velocity error at the initial stage of the motor is 0.002 m/s for the fixed boundary layer and 0.0002 m/s for the adaptive boundary layer. During the motor stabilization phase, the velocity error range is 0m/s-0.014m/s for the fixed boundary layer and 0m/s-0.0002m/s for the adaptive boundary layer. As a result, the adaptive boundary layer control method has a smaller speed error range and better steady state performance of the system.

In Fig.5, a represents MFSMC with fixed boundary layer, b represents MFSMC with adaptive boundary layer.

VI. ANALYSIS OF EXPERIMENTAL RESULTS

The experimental platform is shown in Fig. 6. It consists of the host computer, emergency stop button, PMSLM, servo driver, and scale.

Among them, the experimental platform motor parameters and working conditions are shown in Table 2.

To verify the effectiveness of the designed control strategy, the experimental conditions are made to match the simulation settings.

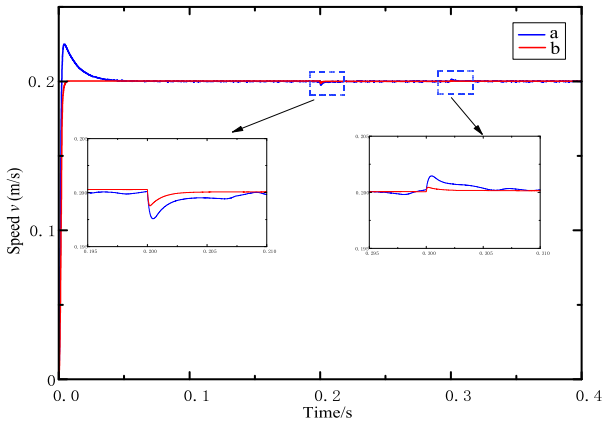

FIGURE 4. Linear speed response curve.

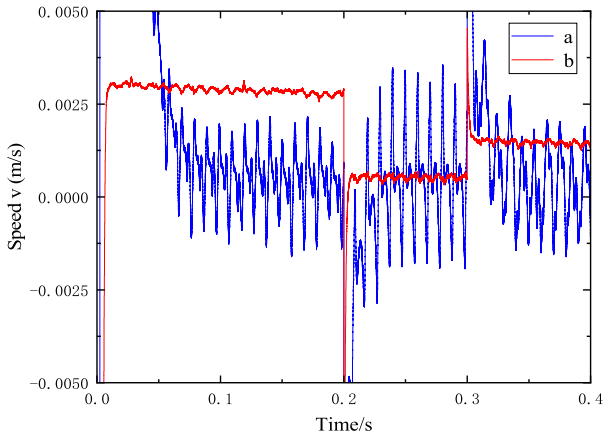

FIGURE 5. Speed error curve considering parameter perturbation.

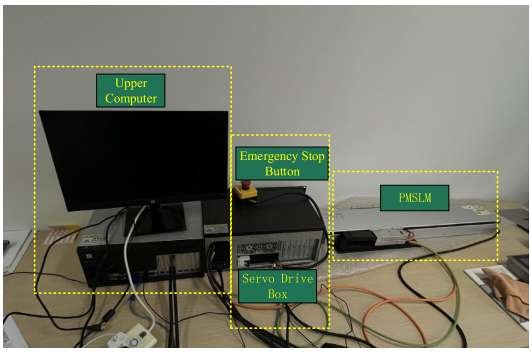

FIGURE 6. Experimental platform.

In the experiment, the grating scale is used to obtain the actual speed of the motor, and the data of the actual speed and the waveform of the observed value are exported through the upper computer. And with the help of MATLAB simulation software to draw the corresponding waveform.

From the Fig. 7, it can be seen that the initial peak of LESO is very high during the motor startup phase, reaching about 108 N, but TMLESO is only 25 N. Second, the LESO took longer than the TMLESO to return to a steady state both when a 100N load was added suddenly and when a load was subtracted suddenly. Therefore, TMLESO not only

TABLE 2. Experimental platform motor parameters and working conditions.

Parameter and unit	Value
rated voltage V	220
peak power W	390
continuous power W	130
peak force N	390
continuous thrust N	130
busbar voltage V	310
sampling time μs	10
coefficient of viscous friction B_m/N·m·s	0.052
static resistance N	10
polar logarithm mm	4
polar distance mm	32
magnetic link Wb	0.048
kinetochore mass Kg	0.3
prime quality Kg	3.96
P-P resistors Ω	3
P-P inductors mH	15.8

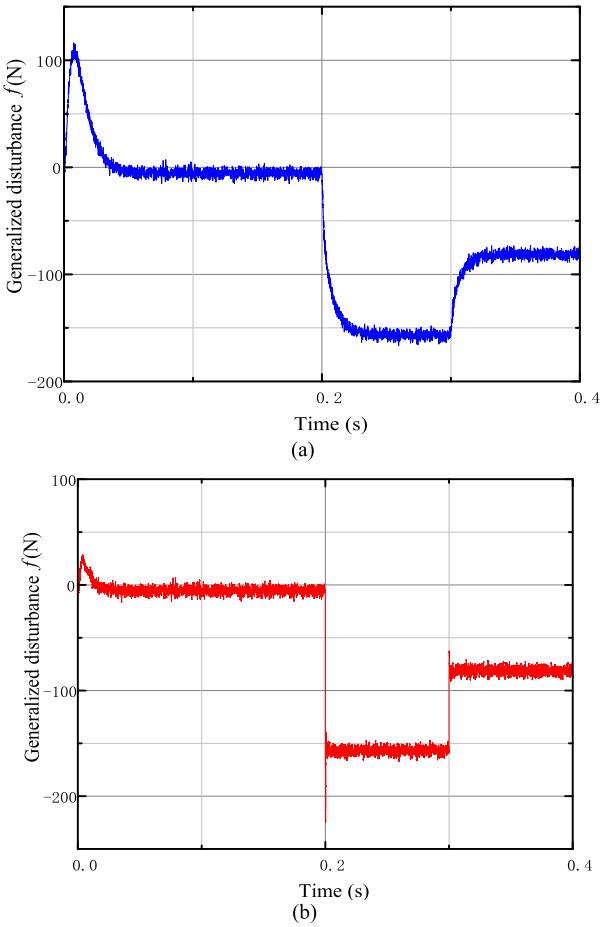

FIGURE 7. Experimental observation curves for generalized perturbations (a)LESO (b)TMLESO.

suppresses the peak at the initial moment well, but also improves the dynamic response speed compared to LESO.

From the Fig.8, it can be seen that the velocity error of the MFSMC with fixed boundary layer in the motor stabilization stage is 0m/s-0.0025m/s,while the velocity error of the MFSMC with adaptive boundary layer is 0m/s-0.05m/s. The velocity error of the MFSMC with the adaptive boundary layer is smaller than that of the MFSMC with the fixed

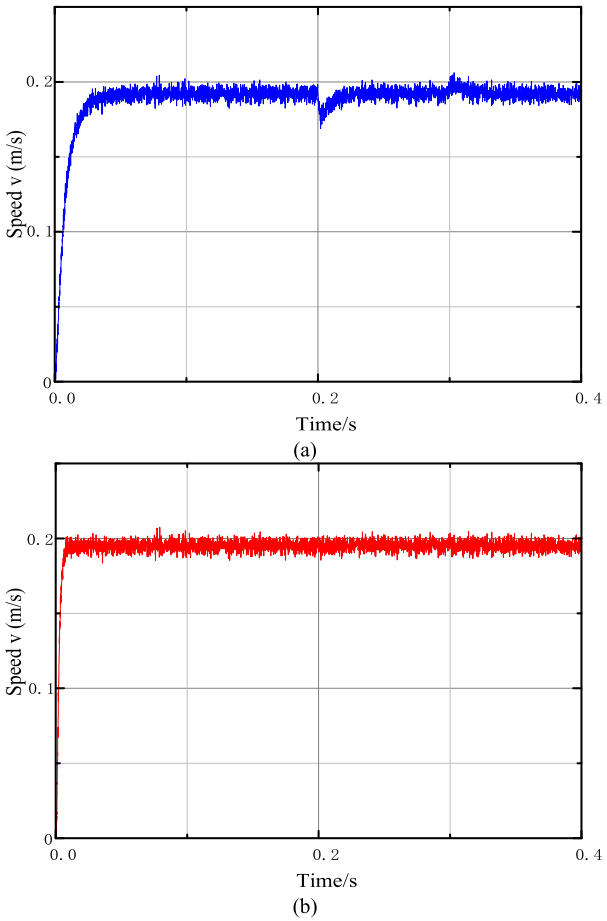

FIGURE 8. Experimental response curve for linear velocity (a) MFSMC with fixed boundary layer (b)MFSMC with adaptive boundary layer.

boundary layer at both 0.2 s sudden load increase and 0.3 s sudden load decrease. This shows that the adaptive MFSMC reduces the velocity error and improves the steady state performance of the system.

In summary, the control strategy proposed in this paper can effectively improve the dynamic performance and control accuracy of the system.

Given the existence of external factors such as air resistance and friction in the actual working conditions. It can be considered that the experimental results are basically consistent with the simulation results, proving the effectiveness of the proposed control strategy.

VII. CONCLUSION

In this paper, we propose a PMSLM speed control method that combines TMLESO and an improved model-free sliding mode controller. The key innovations are: (1) The internal parameter perturbation of the motor is taken into account in the design of the observer, which improves the observation accuracy of the generalized perturbation, while the time-varying function is designed to solve the problem of the initial perturbation peak being too large. (2) A switching function with adaptable boundary layer thickness is used in the velocity sliding mode controller to weaken the inherent jitter of the sliding mode control and improve the velocity tracking performance. The effectiveness of the proposed scheme is verified by MATLAB simulations and experiments on the PMSLM drive system.

In the following work, the focus will be on the current loop intelligent control of PLSLM to further enhance the speed control performance.

REFERENCES

[1] Z. Li, S. Feng, J. Wang, S. Wang, K. Wang, X. Guo, and H. Sun, "Design of model-free position controller for PMSLM based on hyperlocal model," *Electr. Eng.*, vol. 105, no. 4, pp. 2361–2372, Aug. 2023.

[2] Q. Meng and G. Bao, "A novel low-complexity cascaded model predictive control method for PMSM," *Actuators*, vol. 12, no. 9, p. 349, Aug. 2023.

[3] Z. Li, J. An, Q. Zhang, H. Liu, and H. Sun, "Design of PMSLM position controller based on model predictive control algorithm," *IEEE Access*, vol. 9, pp. 78835–78846, 2021.

[4] Q. Wangliang, "Model-free super-twisting sliding mode control of permanent magnet synchronous linear motor based on super-twisting sliding mode observer," *Proc. SPIE*, vol. 12748, pp. 1173–1178, Aug. 2023.

[5] L. Zhang, H. Li, L. Shan, L. Zhang, and L. Zhang, "Double-hierarchical fuzzy exponential convergence law fractional-order sliding mode control for PMSM drive control in EV," *Eng. Sci. Technol., Int. J.*, vol. 47, Nov. 2023, Art. no. 101536.

[6] P. Wang, Y. Xu, R. Ding, W. Liu, S. Shu, and X. Yang, "Multi-kernel neural network sliding mode control for permanent magnet linear synchronous motors," *IEEE Access*, vol. 9, pp. 57385–57392, 2021.

[7] H. Jin, X. Zhao, and T. Wang, "Novel load disturbance observer-based global complementary sliding mode control for a precision motion stage driven by PMLSM," *Int. J. Control, Autom. Syst.*, vol. 19, no. 11, pp. 3676–3687, Nov. 2021.

[8] Y. Yue, Y. Geng, and W. Wang, "Continuous nonsingular fast terminal sliding mode control for speed tracking of PMSM based on finite time disturbance observer," *Processes*, vol. 10, no. 7, p. 1407, Jul. 2022.

[9] C. A. Agustin, J.-T. Yu, Y.-S. Cheng, C.-K. Lin, and Y.-W. Yi, "A synchronized current difference updating technique for model-free predictive current control of PMSM drives," *IEEE Access*, vol. 9, pp. 63306–63318, 2021.

[10] X. Li, Y. Wang, X. Guo, X. Cui, S. Zhang, and Y. Li, "An improved model-free current predictive control method for SPMSM drives," *IEEE Access*, vol. 9, pp. 134672–134681, 2021.

[11] F. Niu, X. Wang, S. Huang, X. Huang, L. Wu, K. Li, and Y. Fang, "Current prediction error reduction method of predictive current control for permanent magnet synchronous motors," *IEEE Access*, vol. 8, pp. 124288–124296, 2020.

[12] X. Wu, Z. Zhu, X. Liu, and F. Yu, "Model-free predictive current control for IPMSMs with multiple current difference updating technique," *J. Power Electron.*, vol. 21, no. 3, pp. 574–582, Mar. 2021.

[13] J. Yuan, J. Li, and Y. Ding, "Modified modeling and internal model control method of thrust ripples in PMLSMs for ultraprecision air-bearing linear feed systems," *Precis. Eng.*, vol. 85, pp. 102–112, Jan. 2024.

[14] T. Satheesh et al., "Unified synchronization and fault-tolerant anti-disturbance control for synchronization of multiple memristor-based neural networks," *Int. J. Robust Nonlinear Control*, vol. 54, no. 2, pp. 405–422, 2023.

[15] R. Sakthivel, T. Satheesh, S. Harshavarthini, and D. J. Almakhles, "State estimation-based robust control design for periodic piecewise systems with time-varying delays," *Int. J. Syst. Sci.*, vol. 54, no. 2, pp. 405–422, Jan. 2023.

[16] Y. T. Chang, C. C. Wen, S. W. Lin, and Y. C. Chen, "Sliding mode control for the dual-excited and steam-valving control of synchronous generator," *Appl. Mech. Mater.*, vols. 284–287, pp. 2320–2324, Jan. 2013.

[17] A. Buja, L. Brown, A. K. Kuchibhotla, R. Berk, E. George, and L. Zhao, "Models as approximations II: A model-free theory of parametric regression," *Stat. Sci.*, vol. 34, no. 4, pp. 1–12, Nov. 2019.

[18] Z. Sun, Y. Deng, J. Wang, H. Li, and H. Cao, "Improved cascaded model-free predictive speed control for PMSM speed ripple minimization based on ultra-local model," *ISA Trans.*, vol. 143, pp. 666–677, Dec. 2023.

[19] W. Xu, A. K. Junejo, Y. Tang, M. Shahab, H. U. R. Habib, Y. Liu, and S. Huang, "Composite speed control of PMSM drive system based on finite time sliding mode observer," *IEEE Access*, vol. 9, pp. 151803–151813, 2021.
[20] S. Du, S. Wang, Y. Wang, L. Jia, W. Sun, and Y. Liu, "Design of sensorless control system for permanent magnet linear synchronous motor based on parametric optimization super-twisting sliding mode observer," *Electronics*, vol. 12, no. 12, p. 2553, Jun. 2023.
[21] Y. Xu, C. Wang, W. Yuan, Z. Li, and Z. Yin, "Anti-disturbance position sensorless control of PMSM based on improved sliding mode observer with suppressed chattering and no phase delay," *J. Electr. Eng. Technol.*, vol. 18, no. 4, pp. 2895–2907, Jul. 2023.
[22] Y. Li, D. Wang, and S. Zhou, "Moment of inertia identification for PMSM based on extended SMO and improved RBFNN," *Energy Rep.*, vol. 9, pp. 521–528, Mar. 2023.

JIAN LIN was born in May 1971. He is a Professor and a Master Tutor. He is the Director of the Automation Teaching and Research Department, Nanjing University of Engineering. His research interests include motor control technology and linear servo system for CNC machine tools.

WUJIE JIANG is currently pursuing the degree with the Nanjing Institute of Technology. His research interests include compound intelligent control methods for permanent magnet synchronous linear motors and servo control.

LEI ZHOU received the B.E. degree in automatic control and the M.S. and Ph.D. degrees in control theory and control engineering from Southeast University, Nanjing, Jiangsu, in 2000, 2005, and 2014, respectively. She joined the Nanjing Institute of Technology, where she is currently a Professor with the School of Automation. Her research interests include predictive control, intelligent control, servo system control, and its applications.

JITING SUN is currently pursuing the degree with the Nanjing Institute of Technology. Her research interest includes compound intelligent control methods for permanent magnet synchronous linear motors.

XINYI SONG is currently pursuing the degree with the Nanjing Institute of Technology. Her research interest includes compound intelligent control method for permanent magnet synchronous linear motor.